

Correlated Transmission and Detection of Concentration-Modulated Chemical Vapor Plumes

Pratistha Shakya, Eamonn Kennedy, Christopher Rose, *Fellow, IEEE*, and Jacob K. Rosenstein, *Senior Member, IEEE*

Abstract—We present an experimental system designed to explore vapor propagation and detection limits with temporally-correlated chemical plumes. By introducing non-random temporal structure into a chemical source, we can apply correlated detection to statistically identify unique concentration-modulated patterns over meter-scale distances, at frequencies up to 100 Hz, and at concentrations at least 2 orders of magnitude below the nominal limit of detection (LOD) of a given sensor. As an illustration of these concepts, we detect 1 ppb modulated isopropanol vapor in a >1 ppm ambient volatile organic compound (VOC) background, using non-selective photoionization detectors (PIPs) having a nominal sensitivity of only 100 ppb. We aim to extend these concepts more broadly to improve the sensitivity and reliability of low-cost chemical sensor networks.

Index Terms—gas sensing, vapor detection, chemical modulation, sensor network, photoionization detector

I. INTRODUCTION

Detecting trace chemicals in natural environments is challenging due to the small amounts of target chemical available to the sensor in presence of comparatively high background interference and highly complex airflows. There are numerous industrial and public safety applications of ambient chemical sensors, such as the identification of toxic and explosive volatile organic compound (VOC) vapors [1], [2]. Additionally, prolonged exposure to VOCs like benzene, butadiene, and toluene poses health risks [3]–[6]. While there are numerous commercial sensors to detect gaseous organic vapors, detecting trace chemicals in natural settings frequently challenges the limits of detection of available sensors.

It is widely appreciated that vapor transport in natural environments is dominated by advection [7], and turbulence and boundary layers confound simple models of chemical dispersion [8], [9]. However, there is a significant gap between the complex fluid mechanics of gas transport, and the relatively simple models which are often assumed in sensor network designs and chemical communications channels [10]. Although it can be difficult to predict *a priori* where a plume will travel, chemical vapors can remain highly concentrated within the plume structure for quite some distance. For example, it has often been observed that insects and animals are able to follow chemical plumes over very long distances [11]. These facts have important implications in the design of distributed chemical sensors and microsystems (Fig. 1) [12]–[19]. Several studies have also analyzed the stochastic and

This work was supported by a grant from the Defense Advanced Research Projects Agency (DARPA), and a Brown University Research Seed Award.

The authors are with the School of Engineering, Brown University, Providence, RI 02912, USA (e-mail: pratistha_shakya@brown.edu, jacob_rosenstein@brown.edu).

Manuscript received date; revised date.

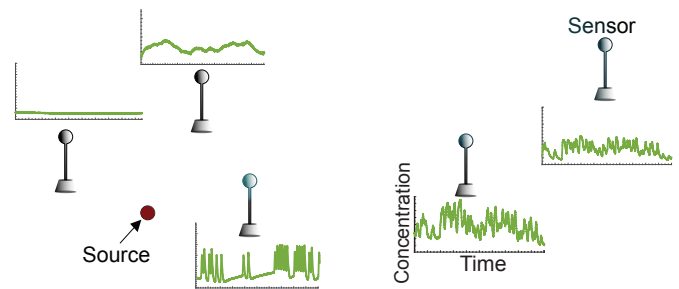


Fig. 1. Distributed sensor networks can be deployed to detect chemical vapors in numerous applications, but reliable detection is challenging due to highly non-uniform dispersion of chemicals from a point source.

time-varying properties of sensor signals to identify unique fluctuation profiles that reveal information about the vapor source [20], [21]. These complex contextual signal fluctuations have been leveraged to improve the sensitivity and selectivity of gas sensors [22]–[26].

In this paper, we introduce a practical and high-performance system for exploring temporally-modulated chemical vapor sensing at a macroscopic scale. By asserting control of the chemical transmission, we introduce structural information into gas sensor datasets, which can assist with studies of chemical transport and improve our ability to reliably identify and localize chemical sources without requiring fine-grained fluid mechanical models. Using these principles, we demonstrate enhanced chemical vapor detection at meter-scale distances and at parts-per-billion analyte concentrations.

II. FUNDAMENTALS FOR SIGNAL PROCESSING

The modulated chemical signal is a sequence of pulses that can be represented as

$$x(t) = \sum_j b_j p(t - j\Delta) \quad (1)$$

where $p(t)$ is a single pulse waveform, Δ is the bit interval, and $b_j \in (0, 1)$ is the j^{th} digit of a binary sequence.

For simplicity we assume chemical transport through the channel is linear and time-invariant, so that the output at sensor n is given by $x(t)$ convolved with an impulse response $h_n(t)$, plus some noise $w_n(t)$. We can express this as

$$y_n(t) = \int_0^\infty h_n(\tau)x(t - \tau)d\tau + w_n(t) \quad (2)$$

The output $y_n(t)$ can be correlated against $x(t)$ to determine whether or not the chemical signal is present. Assuming stationarity, the cross-correlation function on $[0, T]$ is

$$R_{xy}(\tau) = \frac{1}{T} \int_0^T x(t)y(t + \tau)dt \quad (3)$$

If $x(t)$ has a near-impulse autocorrelation and the noise process $w_n(t)$ is independent of $x(t)$, we should expect to see a single feature in $R_{xy}(\tau)$ which resembles the channel impulse response. Under the same assumptions, signal power and noise power can be approximated by

$$\mathcal{P}_{\text{noise}} = N_0 \mathcal{P}_x \quad (4)$$

$$\mathcal{P}_{\text{signal}} = T \mathcal{P}_x^2 \int_0^T h_n^2(t)dt \quad (5)$$

where \mathcal{P}_x is the average power of $x(t)$ in $[0, T]$, N_0 is the noise power spectral density of $w_n(t)$. Assuming T is large relative to the duration of the impulse response $h_n(t)$, we can define the quantity $\mathcal{E}_h = \int_0^T h_n^2(t)dt$ as the (unitless) energy in the impulse response. From this, the signal-to-noise ratio (SNR) of this cross-correlation can be derived as

$$\text{SNR} = \frac{\mathcal{E}_{\text{signal}}}{\mathcal{E}_{\text{noise}}} = T \frac{\mathcal{P}_x \mathcal{E}_h}{N_0} \quad (6)$$

The implication of equation (6) is that detection will improve as more analyte arrives at the sensor, and that since $w_n(t)$ is uncorrelated to $x(t)$, an increased correlation time (T) will improve the cross-correlation SNR. This principle has been used extensively in signal detection in wireless communications systems.

It is also important to consider the frequency response of a system. In noisy systems, the magnitude-squared coherence spectrum $C_{xy}(f)$ between the transmitted and received signals is a convenient metric. For frequencies where the coherence is approximately 1, the output can be predicted by a linear transformation of the input signal; otherwise, the system is partially non-linear, time varying, or noisy at that frequency [27]. The coherence can be expressed as a function of the power spectral densities (P_{xx} , P_{yy}) and cross power spectral densities (P_{xy}) of the input and output signals as

$$C_{xy}(f) = \frac{|P_{xy}(f)|^2}{P_{xx}(f)P_{yy}(f)} \quad (7)$$

III. EXPERIMENTAL PLATFORM

The experimental setup is comprised of an electronically-controlled chemical vapor transmitter and several chemical sensors arranged within a benchtop air flow tube, with the windspeed controlled by a small fan. Several system parameters can be adjusted electronically, including the chemical transmission pattern and the wind velocity. The data presented here utilizes isopropyl alcohol (IPA) vapor as the analyte, though it is compatible with many different chemicals. The overall system is illustrated in Fig. 2. This configuration shares characteristics with systems that other groups have used to study the temporal properties of insect olfactory organs [28], [29].

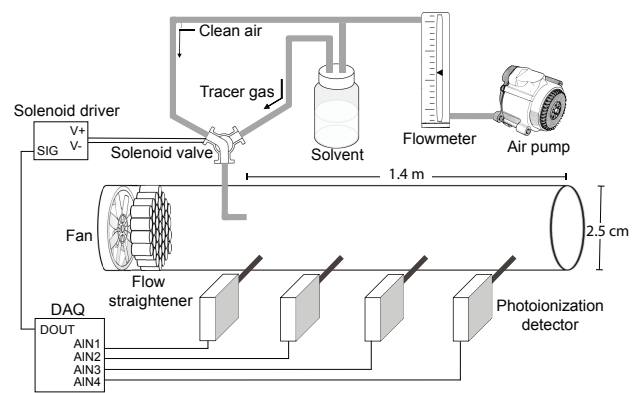


Fig. 2. Benchtop experimental setup for correlated chemical plume experiments. Chemical vapors are released in an electronically-programmable temporal sequence, and their concentration is measured by several high-speed sensors downwind. Figure is not to scale.

A. Transmitter

Concentration-modulated chemical plumes are produced by releasing time-encoded pulses of alcohol vapor through an electronically-controlled transmitter. A pressurized air source is fed through an adjustable variable-area flow regulator which controls the eventual flow rate of transmitted chemical. This is directed into the headspace of a bottle containing vapors from the analyte chemical. The output is controlled by a high-speed three-way solenoid valve (LFA series, Lee company), which selectively bypasses the air path through the chemical source bottle. The final transmission is directed into the flow tube parallel to the background air velocity.

A desired binary transmission pattern is converted to a sequence of fixed-width pulses, and sent to a network-attached data acquisition unit (DAQ, LabJack T7) which controls the solenoid. We use binary pulse-skipping modulation for data transmission, where a ‘0’ bit corresponds to clean air, and ‘1’ corresponds to a short chemical vapor pulse. The transmission pattern, pulse width, and modulation frequency are programmable through a simple python script.

B. Channel

The transmitted signal propagates through an acrylic tube with an internal diameter of 2.5 cm. In an analogy to traditional communications systems, we refer to this tube as the channel [30]. Sensors can be distributed along the channel at several distances from the chemical source. The windspeed within the channel can be electronically adjusted between 0.2-1.5 m/s by a small fan placed at one end of the tube.

C. Sensors

Chemical concentration in the channel is measured by several miniature photoionization detectors (200B miniPID, Aurora Scientific). These sensors have a suction pump that draws air through a small tube, past a 10.6 eV ultraviolet lamp which ionizes small organic molecules in the air. These ions are collected as electrical current by a nearby metal electrode. The nature of the sensor makes it relatively non-selective, and

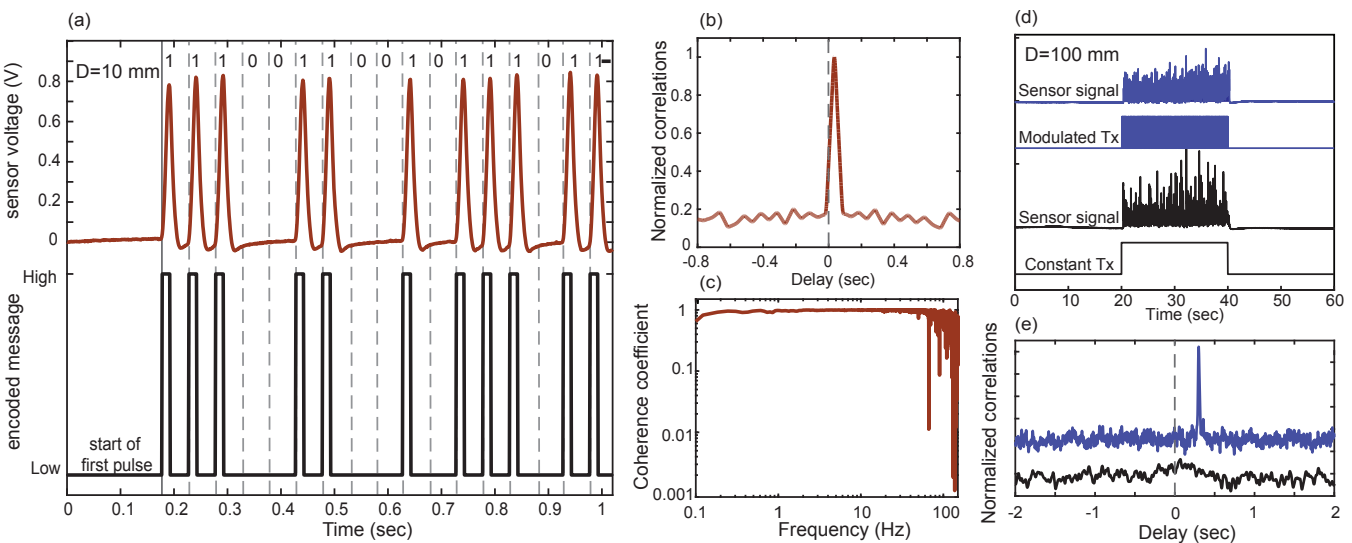


Fig. 3. (a) Transmitted signal (black) and received sensor signal (red) for a bit sequence 11100110010111011 at 20 Hz. Each bit period is indicated by the gray dashed lines. (b) Cross-correlation and (c) magnitude-squared coherence between transmitted pattern and the received signal reveals the presence of the signal and the time-shift information. (d) Comparisons between a chemical transmission modulated at 100 Hz (blue), and a constant transmission (black). In both cases, the sensor output appear to be random fluctuations due to turbulence. (e) Cross-correlation of both sensor signals with the transmission pattern reveals a correlation peak only in the sensor measurement derived from the modulated chemical release (blue).

it responds to all molecules with an ionization potential less than the lamp energy, which generally includes small VOCs (e.g. isopropyl alcohol at 10.1 eV). Scalar sensitivity is higher for compounds with lower ionization potentials. This PID has excellent temporal response with a -3dB frequency of 330 Hz [31]. The amplified output from each sensor is digitized by the DAQ and transferred to a host computer in real time.

IV. RESULTS AND DISCUSSION

A. Signal Detection

Instantaneous concentrations measured by the sensors will inevitably contain noise introduced from turbulence, interfering background chemicals, and electronic noise sources. Since we expect our signal to have a known structure, we can use cross-correlation to measure the similarity between the transmitted and received signals [32]. Cross correlation between signals $x(t)$ and $y(t)$ is given by equation (3).

If the received signal contains the transmitted pattern, we should expect a correlation peak at $\tau = \tau_d$, where τ_d represents a time-shift between the two signals. Fig. 3b shows a normalized cross-correlation between a binary pattern transmitted at 20 Hz, and the output of a sensor at a distance of 10 mm (shown in Fig. 3a). The prominent peak at $\tau = 30$ ms represents the detection of the transmitted pattern. Fig. 3c presents the coherence spectrum, showing that with a 30 percent duty cycle, the system is well behaved to a bandwidth nearing 100 Hz at 10mm.

Fig. 3d presents measurements for a pattern transmitted at 100 bits/sec (blue), alongside a continuous chemical release (black) of similar concentration. Although both received signals are qualitatively similar, only the cross-correlation of the modulated trial yields a clear correlation (Fig. 3e, $\tau_d = 0.3$ sec). We note that air turbulence results in a similar sensor time series even when the chemical is transmitted in a constant non-modulated manner. However, since these fluctuations do not

derive from the modulation pattern, their temporal structure is random and carries no information. Therefore, its cross-correlation with the 100 bit/sec modulation pattern does not have a detection peak.

B. Distance and Windspeed Scaling

We measured the impulse response by transmitting a series of brief (6 ms) pulses through the channel, and calculating the ensemble average of sensor responses at different locations in the channel. Four PID sensors were placed at different distances and sensor voltages were recorded simultaneously. The position-dependent delay (τ_d) is evident in Fig. 4, along with increased pulse spreading with distance. This spreading is caused by diffusion and small-scale turbulence, which disperse the transmitted chemical across larger volumes and reduce the instantaneous concentration.

At longer distances, dispersion reduces the coherence bandwidth. However, increasing windspeed improves the shape of transmitted pulses for a given distance, because diffusion is a strong function of elapsed time rather than distance [33]. Since chemical vapor transport is dominated by advection, if the air velocity is constant then we should expect a simple relationship between the windspeed, distance, and correlation peak according to $\tau_d = \Delta x/v$. Fig. 5 plots the measured signal delays at different sensor positions for three different fan speeds. As expected, these follow a linear trend, and the air velocity can be calculated from the slope.

Previous demonstrations have shown that chemical messages encoded in short vapor pulses can remain coherent over meter-scale distances, for example by recovering a text message sent at 0.33 bits/sec [33], [34]. In contrast, our system can detect modulated binary patterns encoded at rates of up to 50 Hz for comparable distances and windspeeds, as shown in Table I. We observe that reducing the duty cycle of

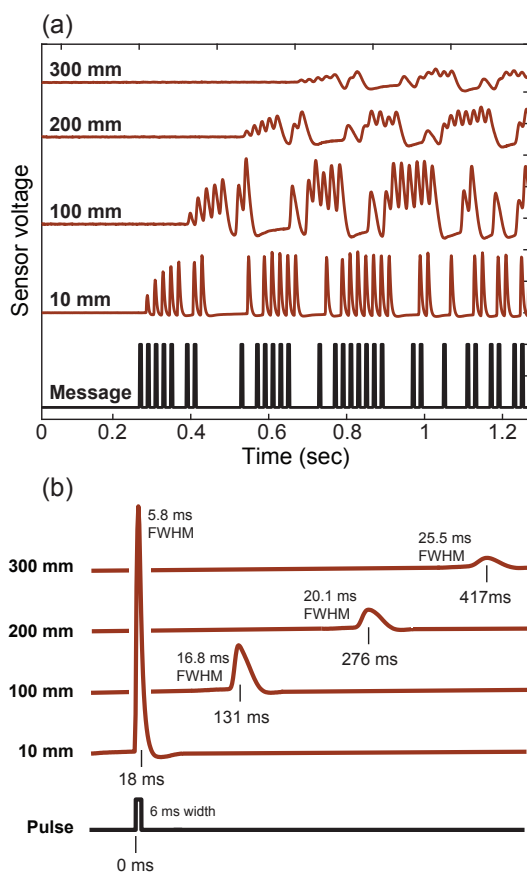


Fig. 4. System response as a function of sensor distance. (a) Observed sensor responses to a 6 ms pulse at four different distances. (b) Ensemble-averaged impulse response at each distance, annotated with the peak delay ($\approx \tau_d$) and full width at half maximum (FWHM).

single pulses yields wider coherence bandwidths and stronger correlation peaks over similar distances and modulation rates. The minimum transmitted pulse width is $\approx 5\text{ms}$, limited by the response time of the solenoid.

C. Enhanced Detection at Low Concentration

Since equation (6) implies that the correlation SNR scales with the correlation duration, we further explored improving the chemical detection limit using longer binary sequences. The Aurora 200B miniPID has a detection threshold of approximately 100 ppb for isopropanol in ambient air. By diluting our liquid isopropanol source more than 10,000-to-1 in deionized water, we were able to produce and detect vapor plumes at concentrations below the background drift of the PID. Background drift in the sensor output depends on a number of environmental and experimental factors including temperature, humidity, and the ambient air composition. Fig. 6a displays sensor signals recorded at a distance of 800 mm with no chemical release (blue), and with a modulated transmission at 40 bits/sec (black). Also shown is the cross-correlation of the transmitted code with each of the sensor signals, after subtracting a two-second moving average. While no correlation peaks are evident in the air background, the modulated signal exhibits a peak at $\tau_d = 2.4\text{s}$.

Correlating against a 5,000 bit sequence at 40 Hz, we were able to detect IPA at average concentrations as low as 1.5

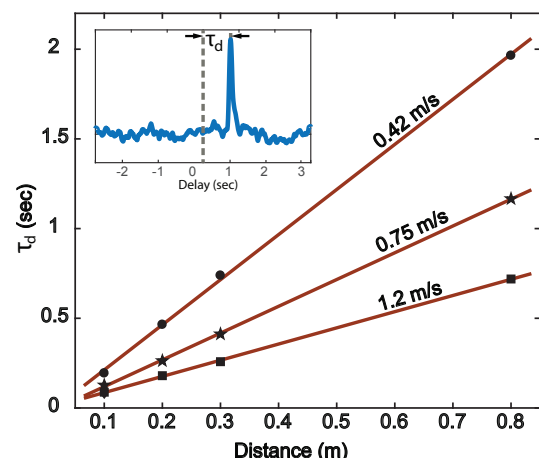


Fig. 5. Observed delay of the correlation peak (τ_d) as a function of sensor position, for three different fan speeds. In constant wind, the delay is linear with position, and the air velocity is calculated from the inverse slope of the linear fit.

TABLE I
ISOPROPANOL VAPOR PLUME DETECTION

Ambient Background	Modulation	Estimated LOD	Detection Time
None	None	100 ppb	0.6 ms
	40 bits/sec	1.5 ppb	125 sec
	25 bits/sec	1 ppb	200 sec

ppb, which represents a sensitivity improvement of nearly 2 orders of magnitude (Table I). These results are consistent with the idea that an extended correlation time will improve the cross-correlation SNR, enabling detection of modulated chemical signals at concentrations below the instantaneous noise floor of a chemical sensor. This improvement in SNR comes at a cost of longer time to detection. This strategy would be complementary to other available PID enhancements such as chemically-selective membranes or alternate electrode arrangements [35].

D. Background Rejection

PIDs are relatively non-selective scalar sensors, which makes it challenging to discriminate between analytes with similar ionization potentials, particularly in complex environments. To improve source discrimination, we can take advantage of information contained in the temporal structure of a plume. As a proof of concept, placed an open ethanol container behind the fan shown in Fig. 2, creating a large $> 1000\text{ppb}$ background signal. In the presence of this dominant ethanol background, we repeated our low-concentration plume modulation, and Fig. 6c compares the sensor response with (black) and without (yellow) the modulated IPA. Diluted IPA was modulated at 25 Hz to give a 1 ppb mean concentration at 1.4 meters from the source. Clearly the turbulent 1 ppm ethanol background would frustrate detection of the much weaker IPA concentration. Yet after a simple subtraction of a two-second moving average from the sensor signals, we were able to observe a correlation peak to identify the presence of the IPA plume.

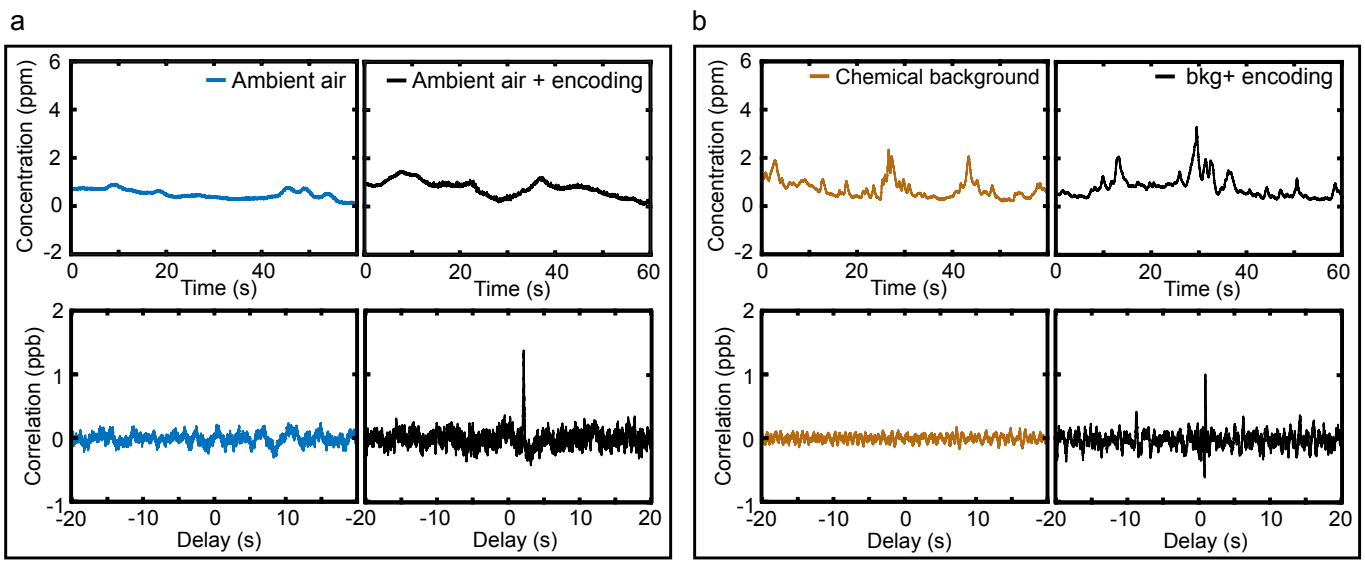


Fig. 6. Modulation-enhanced chemical vapor detection at low concentrations and high background. (a) The top two panels present sensor outputs at 0.8 m recorded with an ambient air background (blue), and with a 40 Hz modulated chemical signal (black), using heavily diluted IPA in deionized water with 1.5 ppb mean concentration. Cross-correlation of each sensor output with the modulation code shows a prominent peak when the signal is present, even at concentrations below the sensor's stated limit of detection. (b) Sensor outputs at 1.4 m recorded with a large ethanol background (yellow) and with a 25 Hz modulated 1 ppb IPA signal in addition to the ethanol background (black). Cross-correlation of the sensor output with the modulation pattern yields a peak at $\tau_d = 0.94$ seconds. No correlation peak is observed for the ethanol background.

This demonstrates the ability of the modulated detection to reject both slow instrument drifts and larger and faster ambient chemical backgrounds. Chemical vapors with known unique temporal structure can be detected at concentrations that are more than 3 orders of magnitude below the background signal, without using a chemically-selective sensor. These results could be used to improve performance in complex systems with multiple chemical sources [34], where reliability tends to be limited by interference.

V. CONCLUSION

We have presented an experimental platform for transmission and detection of temporally-modulated chemical vapor plumes. By correlating measured signals against a known transmitted pattern, we have been able to identify signals at meter-scale distances, using modulation rates as fast as 100 Hz. The testbed allows adjustments of system parameters to better understand the nature of chemical vapor propagation in a controlled environment, which we have used to observe transport delay, dispersion, and coherence that scale with wind velocity and distance. Despite using non-selective scalar sensors, we have demonstrated strong VOC background rejection, as well as ppb chemical detection nearly two orders of magnitude below the nominal detection limit of the sensor. Moving forward, we intend to find mathematical strategies which leverage temporal structure in chemical vapor plumes, and impose or measure unique spatiotemporal fluctuations to further improve the accuracy and reliability of chemical detection and source localization.

ACKNOWLEDGMENT

The authors would like to thank Daniel Harris for helpful discussions and advice.

REFERENCES

- [1] M. J. Lefferts and M. R. Castell, "Vapour sensing of explosive materials," *Anal. Methods*, pp. 9005-9017, 2015.
- [2] A. Nehorai, B. Porat and E. Paldi, "Detection and Localization of Vapor-Emitting Sources," *IEEE Trans. on Signal Process.*, vol. 43, no. 1, 1995.
- [3] R.L. Woodfin (Ed.), *Trace Chemical Sensing of Explosives*, John Wiley and Sons, Hoboken, New Jersey (2007)
- [4] Molhave, L., Bach, B. and Pedersen, O. F. Human reactions to low concentrations of volatile organic compounds. *Environ. Int.* 12, 167175 (1986).
- [5] Andersson, K. et al. TVOC and Health in Non-industrial Indoor Environments. *Indoor Air* 7, 7891 (1997).
- [6] Guo, H., Lee, S. C., Chan, L. Y. and Li, W. M. Risk assessment of exposure to volatile organic compounds in different indoor environments. *Environ. Res.* 94, 5766, doi: 10.1016/s0013-9351(03)00035-5 (2004).
- [7] C. D. Jones, "On the structure of instantaneous plumes in the atmosphere," *J. Hazard. Mater.*, vol. 7, no. 2, pp 87-112, 1983.
- [8] F. A. Gifford, "Statistical properties of a fluctuating plume dispersion model," *Adv. Geophys.*, vol. 6, pp. 117-137, 1959
- [9] J. A. Farrell, J. Murlis, X. Long, W. Li and R. T. Carde, "Filament-Based Atmospheric Dispersion Model to Achieve Short Time-Scale Structure of Odor Plumes," *Environ. Fluid Mech.*, vol. 2, no. 1-2, pp. 143-163, 2002
- [10] N. Farsad, D. Pan, A. Goldsmith and M. Young, "A Novel Experimental Platform for In-Vessel Multi-Chemical Molecular Communications," arXiv:1704.04810, Apr. 2017.
- [11] J. Murlis, J. Elkinton, and R. T. Carde, "Odor Plumes And How Insects Use Them," *Annu. Rev. Entomol.*, vol. 37, no. 1, pp. 505-532, 1992.
- [12] M. Y. Afridi, J. S. Suehle, D. W. Berning, A. R. Hefner, R. E. Cavicchi, S. Semancik, C. B. Montgomery, and C. J. Taylor, "A monolithic CMOS microhotplate-based gas sensor system," *IEEE Sens. J.*, vol. 2, no. 6, pp. 644-655, 2002.
- [13] E. Woolfenden, "Sorbent-based sampling methods for volatile and semi-volatile organic compounds in air: Part 1: Sorbent-based air monitoring options," *J. Chromatogr. A*, vol. 1217, no. 16, pp. 2674-2684, 2010.
- [14] M. L. Johnston, I. Kymmissis, and K. L. Shepard, "FBAR-CMOS oscillator array for mass-sensing applications," *IEEE Sens. J.*, vol. 10, no. 6, pp. 1042-1047, 2010.
- [15] S. Dai, R. T. Perera, Z. Yang, and J. K. Rosenstein, "A 155-dB Dynamic Range Current Measurement Front End for Electrochemical Biosensing," *IEEE Trans. Biomed. Circuits Syst.*, vol. 10, no. 5, pp. 935-944, 2016.
- [16] S. Dai and J. K. Rosenstein, "Relaxation Oscillator for Near-Zero-Power Sensors," *IEEE Custom Integrated Circuits Conference (CICC)*, pp. 4-7, 2015.

- [17] M. M. Shulaker, G. Hills, R. S. Park, R. T. Howe, K. Saraswat, P. Wong, and S. Mitra, "Three-dimensional integration of nanotechnologies for computing and data storage on a single chip," *Nat. Publ. Gr.*, vol. 547, no. 7661, pp. 74-78, 2017.
- [18] B. Raman, D. C. Meier, J. K. Evju, and S. Semancik, "Designing and optimizing microsensor arrays for recognizing chemical hazards in complex environments," *Actuator B-Chem*, vol. 137, np. 2, pp617-629, 2009.
- [19] H. Li, C. S. Boling, and A. J. Mason, "CMOS Amperometric ADC With High Sensitivity , Dynamic Range and Power Efficiency for Air Quality Monitoring," pp. 1-11, 2016.
- [20] E. L. Hines, E. Llobet, and J. W. Gardner, "Electronic noses: A review of signal processing techniques," *IEE Proc.- Circuits, Devices Syst.*, vol. 146, no. 6, pp. 297-310, Dec. 1999.
- [21] L. Lentka et al. "Non-Gaussian Resistance Fluctuations in Gold-Nanoparticle-Based Gas Sensors: An Appraisal of Different Evaluation Techniques." *Sensors (Basel)*, vol. 17, no. 4 , April 2017.
- [22] M. Schmuker, V. Bahr, R. Huerta, "Exploiting plume structure to decode gas source distance using metal-oxide gas sensors," *Sens. Actuators B, Chem.*, vol. 235, pp. 636-646, 2016.
- [23] L. B. Kish et al., "Detecting harmful gases using fluctuation-enhanced sensing with Taguchi sensors," *IEEE Sensors Journal*, vol. 5, no. 4, pp. 671-676, 2005.
- [24] Z. Chen, Y. Zheng, K. Chen, H. Li and J. Jian, "Concentration Estimator of Mixed VOC Gases Using Sensor Array With Neural Networks and Decision Tree Learning," *IEEE Sensors Journal*, vol. 17, no. 6, pp. 1884-1892, 2017.
- [25] A. Vergara, J. Fonollosa, J. Mahiques, M. Trincavelli, N. Rulkov and R. Huerta, "On the performance of gas sensor arrays in open sampling systems using Inhibitory Support Vector Machines," *Sens. Actuators B, Chem.*, vol. 185, pp. 462-477, 2013.
- [26] J. G. Monroy, A. Lilienthal, J. L. Blanco, J. Gonzlez-Jimenez and M. Trincavelli, "Calibration of MOX gas sensors in open sampling systems based on Gaussian Processes," 2012 *IEEE Sensors*, Taipei, 2012, pp. 1-4.
- [27] G. C. Carter, C.H. Knapp, and A.H. Nuttal, "Estimation of the magnitude-squared coherence function via overlapped Fast Fourier Transform Processing," *IEEE Trans. On Audio Electroacoustics*, AU-21, 1973.
- [28] P. Szyszka, R. C. Gerkin, C. G. Galizia and B. H. Smith, "High-speed odor transduction and pulse tracking by insect olfactory receptor neurons," *PNAS*, vol. 111, no. 47 , 2014
- [29] J. Schuckel and A. S. French, "A digital sequence method of dynamic olfactory characterization," *J. Neurosci. Methods*, vol. 171, no. 1, pp. 98-103, 2008.
- [30] N. R. Kim and C. B. Chae, "Novel modulation techniques using isomers as messenger molecules for nano communication networks via diffusion," *IEEE J. Sel. Areas Commun.*, vol. 31, no. 12, pp. 847-856, 2013.
- [31] M. M. Metzger and J. C Klewicki, "Development and characterization of a probe to measure scalar transport," *IOP Meas. Sci. Technol.* , vol. 14, no. 8, pp. 1437, 2003
- [32] G. F. Kirkbright and R M. Miller, "Cross-Correlation Techniques for Signal Recovery in Thermal Wave Imaging," *Anal. Chem*, vol. 55, no. 3, 1983.
- [33] N. Farsad, W. Guo, A. W. Eckford and K. Elissa, "Tabletop Molecular Communication: Text Messages through Chemical Signals," *PLOS ONE*, vol. 8, no. 12, 2013.
- [34] B. H. Koo, C. Lee, H. B. Yilmaz, N. Farsad, A. Eckford and C. B. Chae, "Molecular MIMO: From Theory to Prototype," in *IEEE Journal on Selected Areas in Communications*, vol. 34, no. 3, pp. 600-614, March 2016.
- [35] Spinelle L, Gerboles M, Kok G, Persijn S, Sauerwald T. "Review of Portable and Low-Cost Sensors for the Ambient Air Monitoring of Benzene and Other Volatile Organic Compounds," *Sensors (Basel, Switzerland)*. 2017.



Pratistha Shakya received the M.Sc. degree in electrical engineering from Brown University, Providence, RI, USA and the B.Sc. degree in electrical engineering from Trinity College, Hartford, CT, USA, in 2017 and 2015 respectively.

She is currently working toward the Ph.D. degree in electrical engineering and computer science at Brown University. Her research interests include distributed sensor networks and sensor system design.



Eamonn Kennedy is a Postdoctoral Research Associate in the Rosenstein laboratory in the School of Engineering at Brown University. Following his BSc in Physics in University College Dublin in 2010 and an MSc in near-field optics, he completed his PhD in the UCD Nanophotonics Research Group in 2014. He was a Postdoctoral Fellow in the Timp Lab at Notre Dame from 2014 to 2017.

His research interests include infrared biosensing at the nanoscale, liquid cell electron microscopy, nanopores and single molecule sequencing.



Jacob K. Rosenstein is currently an Assistant Professor in the School of Engineering at Brown University. He received the Ph.D. degree in electrical engineering from Columbia University in 2013.

He worked as a systems engineer in the Wireless division at Analog Devices and MediaTek Wireless from 2005 to 2008, contributing to the SoftFone line of cellular baseband chipsets. Current research interests include mixed signal circuit design, biomolecular sensors, chemical sensor networks, and biomedical electronics.



Christopher Rose received the Ph.D. degree in EECS from the Massachusetts Institute of Technology, Cambridge, MA, in 1985.

He worked as a Technical Staff Member at AT&T Bell Laboratories Research from 1985 to 1990. From 1990 to 2015, he was with the Wireless Information Network Laboratory, Department of Electrical and Computer Engineering, Rutgers University, as a Founding Member. Currently, he is a Professor of Engineering at Brown University. His research interests include molecular communication and communication/information theory as a lens on everything.